

## Original Article

Effect of *Rhazya stricta*-synthesized Copper Nanoparticles on *Staphylococcus aureus*-infected Wounds in Rabbit

Ali Hussein Aldujaily<sup>1</sup> , Kifah Fadhil Hassoon<sup>2</sup> , Douaa Barzan Salman<sup>2</sup>, Ghadeer Sabah Bustani<sup>3\*</sup>

1. Department of Veterinary Clinical Sciences, Faculty of Veterinary Medicine, University of Kufa, Kufa, Iraq.

2. Department of Veterinary Microbiology, Faculty of Veterinary Medicine, University of Kufa, Kufa, Iraq.

3. Department of Anesthesia, Faculty of Medical Technologies, The Islamic University, Najaf, Iraq.



**How to Cite This Article** Aldujaily, A. H., Hassoon, K. F., Salman, D. B., & Bustani, Gh. S. (2025). Effect of *Rhazya stricta*-synthesized Copper Nanoparticles on *Staphylococcus aureus*-infected Wounds in Rabbit. *Iranian Journal of Veterinary Medicine*, 19(2), 211-226. <http://dx.doi.org/10.32598/ijvm.19.2.1005593>

<http://dx.doi.org/10.32598/ijvm.19.2.1005593>

## ABSTRACT

**Background:** Nanoparticles (NPs) are utilized in various technological fields, including medicine, due to their inherent antibacterial properties. Recent research has focused on the biosynthesis of copper NPs (CuNPs) and their potential medical applications.

**Objectives:** This study aimed to use *Rhazya stricta* for the green synthesis of CuNPs and assess their effectiveness in eradicating bacterial pathogens, particularly *Staphylococcus aureus*, and promoting wound healing in rabbits.

**Methods:** The synthesized NPs were characterized using UV-visible spectroscopy, scanning electron microscopy (SEM), energy dispersive spectroscopy (EDS), x-ray diffraction (XRD), atomic force microscopy (AFM), and zeta potential analysis. Fifteen rabbits were divided into three groups of five. Full-thickness costo-abdominal skin wounds were created on the right side of each rabbit. The first group served as the untreated control, the second group was treated with CuNPs, and the third group received fusidic acid treatment.

**Results:** *R. stricta* extract successfully synthesized CuNPs. The application of CuNPs on *S. aureus*-contaminated wounds showed faster healing than fusidic acid treatment. The CuNPs group healed in 16 days, while the fusidic acid group healed in 22 days. CuNPs-treated wounds had significantly reduced wound area, total cell count, neutrophil count, macrophage count, and lymphocyte count ( $P < 0.05$ ), along with increased wound contracture ( $P < 0.05$ ). Bacterial counts indicated that CuNPs eradicated *S. aureus* infections in seven days, compared to 12 days for fusidic acid. CuNPs reduced inflammation and promoted collagen fiber deposition, leading to better healing of *S. aureus*-infected wounds by decreasing hemorrhagic regions and inflammatory cells.

**Conclusion:** CuNPs synthesized using *R. stricta* show promising potential as a safe and effective treatment for infected wounds. They effectively eradicate infections and promote efficient wound healing, making them a viable therapeutic option for managing infected wounds.

**Keywords:** *Rhazya stricta*, Copper nanoparticles (CuNPs), *Staphylococcus aureus*, Skin wounds, Histopathology, Rabbits

### Article info:

Received: 26 Sep 2024

Accepted: 28 Sep 2024

Publish: 01 Apr 2025

### \* Corresponding Author:

Ghadeer Sabah Bustani, Associate Professor.

Address: Department of Anesthesia, Faculty of Medical Technologies, The Islamic University, Najaf, Iraq.

Phone: +964 (772) 8299090

E-mail: [Bustani@iu Najaf.edu.iq](mailto:Bustani@iu Najaf.edu.iq)



Copyright © 2025 The Author(s);

This is an open access article distributed under the terms of the Creative Commons Attribution License (CC-BY-NC: <https://creativecommons.org/licenses/by-nc/4.0/legalcode.en>), which permits use, distribution, and reproduction in any medium, provided the original work is properly cited and is not used for commercial purposes.

## Introduction

The process of wound healing is a multifaceted and intricate reaction that involves various stages, such as platelet accumulation, coagulation, inflammatory response to injury, modification of the underlying materials, angiogenesis, and re-epithelization (Huimin et al., 2023). The presence of pathogens in a wound can impede the healing process and increase the risk of sepsis, a serious medical condition. Chronic wounds provide an optimal environment for the development of mature biofilms, which offer bacteria protection against the impact of antibiotics and the body's immune proteins (Razdan et al., 2022; Bustani & Kashef Alghetaa, 2024).

The bacterium *Staphylococcus aureus*, commonly referred to as *S. aureus*, has been recognized as a prominent etiological agent responsible for wound infections. This pathogen possesses the capacity to acquire resistance to multiple antibiotics, thereby exacerbating the challenge of effectively treating chronic infections (Foroutan et al., 2022; Pal et al., 2023).

The utilization of nanotechnology in the field of medicine is increasingly prevalent, leading to its application in addressing the challenge of antibiotic resistance. Bioactive nanoparticles (NPs) represent a prominent category of nanomaterials that are being explored for potential clinical applications. These NPs possess several advantageous characteristics, including cost-effectiveness, a significant surface-to-volume ratio, exceptional stability, and a high level of safety (Samuel et al., 2022; Hossieni et al., 2024).

Copper NPs (CuNPs) have garnered significant attention due to their diverse range of applications, including their use as antibacterial and antifungal agents, as well as their antioxidant properties and ability to prevent biofilm formation in the fields of biotechnology and bioengineering (Zhang et al., 2023). CuNPs can be synthesized through diverse methodologies, encompassing physical, chemical, and biological approaches. Biological environmentally friendly approaches are preferred over alternative methods (Hasanin et al., 2021).

The selection of plant materials for biosynthesis is based on the presence of reducing agents, such as ascorbic acid and phenolic compounds, which have been identified as potentially important factors in the synthesis of metal NPs (Islam et al., 2022). *R. stricta* exhibits a significant abundance of diverse phytoconstituents, encompassing flavonoids, steroids, tannins, saponins,

glycosides, terpenoids, coumarins, and beta-cyanins. These phytoconstituents exhibit diverse pharmacological activities, including antioxidant, anti-inflammatory, and anti-cancer properties (Rahman et al., 2023; Rahchamani et al., 2024).

Numerous studies conducted in recent years have established the efficacy of CuNPs as agents for wound healing, offering a protective barrier against infections. CuNPs induce angiogenesis, the process of new blood vessel formation, at the site of the wound. In addition, they also induce the upregulation of vascular endothelial growth factor (VEGF), which promotes the transportation of various nutrients and the formation of collagen, both of which are essential for wound healing (Gaddafi et al., 2023; Yaşayan et al., 2023).

The primary objective of this study was to investigate the effects of CuNPs synthesized by *R. stricta* on surgically induced full-thickness skin wounds in rabbits that were intentionally infected with *S. aureus*.

## Materials and Methods

### Study design

The study was conducted in two distinct phases. The initial phase focused on the biosynthesis of CuNPs using *R. stricta*. In the subsequent phase, *S. aureus* was isolated from contaminated wounds of dogs. Then, skin wounds on rabbits were infected with *S. aureus* and subsequently treated with CuNPs. The animal's gender was not considered in this investigation because the medication was applied externally to the skin, and there was no observed difference in skin healing between males and females.

### Production of CuNPs

#### Plant collection

The researchers collected the leaves and stems of *R. stricta* from the arid region of Al-Najaf in Iraq. The specimen was collected and verified at the Herbal Center for Scientific Authentication, located within the Department of Physiology and Pharmacology at the Faculty of Pharmacy, University of Kufa, Kufa, Iraq.

#### Plant extraction

The leaves of *R. stricta* were collected and subjected to two rounds of washing with distilled water to remove any dust particles. Subsequently, the leaves were air-dried in the shade at room temperature. The dried leaves, weighing 25 grams, were fragmented and intro-

duced into an Erlenmeyer flask containing 250 mL of sterile distilled water. The flask was heated to 90 °C in a water bath (Gallen Kamp; England) for 45 minutes. In order to generate the aqueous plant extracts, the extract underwent filtration using Whatman No. 1 filter paper, followed by centrifugation at a speed of 3000 rpm for 10 minutes (Awwad et al., 2013). In order to ensure the absence of contamination in the prepared extracts, a volume of 0.1 mL of the plant extract was acquired and cultivated on nutrient agar. Subsequently, the agar plates were incubated at 37 °C for 24 hours.

### Biosynthesis of CuNPs

Following the filtration process mentioned above, 25 ml of each aqueous extract was individually introduced into a 250 mL Erlenmeyer flask containing 100 mL of a 0.01 M CuSO<sub>4</sub> solution. This sequential addition was carried out for 10-15 minutes. The flask's contents were agitated using a magnetic stirrer operating at a rotational speed of 150 rpm and maintained at 30 °C. The production of CuNPs was deemed complete when a transition in color occurred, shifting from a light yellow hue to a dark green shade. This change was attributed to the surface plasmon resonance (SPR) phenomenon, which resulted in a peak at the wavelength range of 550-600 nm as observed using a UV-visible spectrophotometer (Shimadzu; Japan). The sample was then subjected to centrifugation at 6000 rpm for 15 minutes. The resulting supernatant was then discarded and replaced with deionized distilled water. Subsequently, the sample was centrifuged three additional times at the same speed and duration to ensure the complete removal of any remaining supernatant. The resulting pellet was then stored overnight in a hot air oven maintained at 60 °C. This process ultimately yielded NP powder (Rani et al., 2020).

### Characterization of CuNPs

The characterization of the samples was conducted using UV-visible spectroscopy. The achievement was accomplished through the evaluation of the UV-visible spectra of the reaction mixture, which underwent periodic dilution with deionized distillation water (Caroling et al., 2013).

The shape and size of the NPs were determined using scanning electron microscopy (SEM) (FEI; Netherlands). The x-ray diffraction (XRD) (Broker; Germany) is a widely employed technique for examining molecular and crystal morphologies, qualitatively identifying chemicals, quantitatively determining chemical species, assessing crystallinity, analyzing isomorphous replacements, and measuring particle sizes (Zhang et al., 2017).

The presence of NPs in point analysis was determined using energy-dispersive x-ray spectroscopy (EDS) (Caroling et al., 2013). Vinelli et al. examined the dispersion and aggregation of nanomaterials, as well as their size and form, through the utilization of atomic force microscopy (AFM) (Vinelli et al., 2008). The stability of the produced NPs was assessed using a zeta potential analyzer (Brookhaven; USA), which measured the zeta potential values ranging from -160 mV to +160 mV. The obtained data were then visualized in graphical form (Raja et al., 2017).

### Experimental study

Laboratory animal initialization fifteen adult domestic rabbits of both sexes (11 male and 4 female) aged 8–10 weeks with an average body weight of 1,800±20 g were fed commercial pellets and grass for seven days prior to the experiment for acclimatization. This acclimatization was conducted from August 2023 to October 2023 in the animal house of the Faculty of Veterinary Medicine at the University of Kufa, Iraq. The animals were randomly divided into three equal groups (n=5).

### Anesthesia and wounding

The rabbits were anesthetized intramuscularly using a ketamine-xylazine-saline solution that contained 40 mg/kg of ketamine (Holland) and 2 mg/kg of xylazine (Belgium) (Cardoso et al., 2020). In brief, the rabbits' hair was removed, and the exposed skin was cleaned with 70% ethanol (APCO; Jordan). Full-thickness skin incisions of 1 cm in diameter were made on the rabbits' thoracoabdominal sides (Figure 1). The exposed wounds received no dressings throughout the experiment (Behera et al., 2019).

### Preparation of bacteria

In the Al-Najaf Teaching Veterinary Hospital, *S. aureus* was isolated from contaminated wounds of dogs. The VITEK-2 (Biomerieux; France) compact automated system was utilized for bacterial identification and antibiogram testing based on the determination of the minimum inhibitory concentration (MIC) technique. According to VITEK-2 compact system, the antibiotic susceptibility test (AST) revealed that the isolated bacteria were resistant to many classes of antibiotics, including benzylpenicillin, oxacillin, tobramycin, moxifloxacin, clindamycin, vancomycin, and tetracycline. Fusidic acid was selected due to the reduced susceptibility of the *S. aureus* isolate to other antibiotics.



**Figure 1.** A rabbit with incisions on its skin

The microorganisms were cultivated in Muller-Hinton broth. After undergoing centrifugation at a speed of 1,000 rpm for 15 minutes, the bacteria were diluted in sterile phosphate-buffered saline to achieve a concentration of  $1 \times 10^8$  CFU/mL. Following wound surgery, 100  $\mu$ l of the bacterial suspension was topically applied to each wound bed (Tanideh et al., 2014).

### Experimental treatments

As mentioned earlier, the rabbits were divided into three distinct groups. There were five animals in each group, and each group was administered the prescribed medication five days subsequent to the initiation of infection. All three animal groups were treated in the following manner:

1. Control group: Non-treated.
2. CuNPs- treated group: Treated with 0.2% CuNP ointment applied daily for five days on the affected skin.
3. Fusidic acid-treated group: Treated with 2% fusidic acid ointment applied daily for five days on the affected skin.

### Data collection

#### Documentation of wound healing time

The duration of wound healing was measured from the moment of wound induction to re-epithelialization. The observations were randomly estimated at intervals of 7, 14, 21, and 28 days until the scar completely disappeared (Mirnezami et al., 2018).

#### Determination of healing rate

At seven-day intervals, the rate of healing for each treatment group was assessed. It was determined by dividing the highest average wound margin distance from the wound's center by the time required for wound closure. The Equation 1 was used to determine the weekly healing rate:

1. Wound closure (%) =  $\frac{(\text{Area of the wound on day 0 (mm)} - \text{Area of the wound on indicated day (mm)})}{\text{Area of the wound on day 0 (mm)}} \times 100$  (Sato et al., 2015)

#### White blood count (WBC) count

The WBC count was conducted using the Vet. Scan HM5 hematology equipment manufactured by ABAXIS Company. The WBC was assessed every week for every treatment group.

#### Histopathological evaluation

On days 3, 7, 14, and 21 of the experiment, a histological test was done to discriminate between these groups by taking 5 mm of the healing regions. Overnight, the skin slices were fixed in a 10% formalin (BDH; England) solution (pH 7.4). They were then processed through a succession of alcohol and xylene grades. Then, the tissues were immersed in paraffin wax at 65 °C. Tissue blocks were cut into 5  $\mu$ m thick slices, stained with hematoxylin and eosin (H&E), and examined under a light microscope (Al Mousaw et al., 2020; Diniz et al., 2020).

#### Statistical analysis



**Figure 2.** Visualization of the green synthesis of CuNPs

A) Before incubation, B) A solution containing CuNPs after incubation

Data were investigated by SPSS Software, version 26 using the one-way ANOVA. The results were presented as Mean $\pm$ SE, and a  $P < 0.05$  was considered statistically significant.

## Results

### CuNPs biosynthesis

Following a 24-hour incubation period, a discernible alteration in color was observed, signifying the occurrence of NP formation within the reaction mixture. The alteration in color of the medium was observed as a transition from a yellow hue to a reddish-brown shade upon the introduction of the plant extracts and  $\text{CuSO}_4$  reaction mixture, conducted in darkness (Figure 2).

### Characterization of CuNPs

#### UV- visible spectroscopy

Confirmation of NP biosynthesis can be achieved through visual observation and the measurement of the SPR band using UV-vis spectroscopy. The presence of a solitary SPR band suggests that the NPs possess a spherical morphology (Badri et al., 2021). The UV-visible spectrogram, as illustrated in Figure 3, demonstrates the

successful synthesis of CuNPs and the presence of their distinctive surface plasmonic resonance peak at a wavelength of 570 nm.

#### SEM analysis

The SEM was employed to validate the morphology and dimensions of the biogenic NPs (Chinnathambi et al., 2021). This study examined the distribution and morphology of biogenic NPs synthesized by *Rhazya stricta*. The CuNPs, which are spherically shaped, exhibit a well-dispersed nature. The average size of these CuNPs was measured to be 15.75 nm (Figure 4).

The SEM images of the CuNPs exhibited an irregular, diminutive spherical morphology. This finding is consistent with the observations reported by Zhao et al. (Zhao et al., 2022).

#### Energy dispersive spectroscopy (EDS) analysis

The EDS technique, specifically point and mapping analysis, was employed to quantitatively assess the presence of NPs by examining the optical absorption peaks of various elements. The elemental analysis of CuNPs synthesized by *R. stricta* revealed the composition of constituent elements, as depicted in Figure 5.

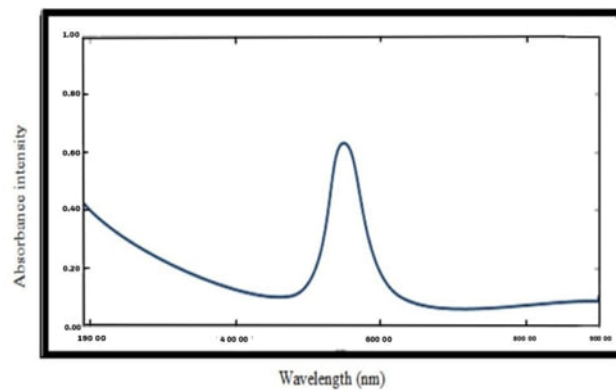


**Figure 3.** UV-visible spectroscopy analysis of CuNPs synthesized by *R. stricta*

The analysis of EDS spectroscopy was conducted on CuNPs synthesized using *R. stricta*, thereby validating the existence of elemental copper through the observed signals. The EDS spectrum exhibited a discernible peak, attributed to the absorption of copper nanocrystallites that corresponded to SPR. The observed component was copper, and additional elements, such as oxygen and carbon, were detected (Bukhari et al., 2021).

#### Atomic force microscope (AFM)

An AFM (Broker; Germany) imaging technique was employed to analyze the synthesis of CuNPs using *R. stricta*. The reported morphology of CuNPs was found to be influenced by the shape of the probe, specifically in relation to its lateral dimensions. The height measurements possess the capability to accurately and precisely determine the elevation of NPs. The CuNPs biosynthesized

from *R. stricta* exhibited an average diameter of 42.21 nm and an average roughness of 11.18 nm (Figure 6).

#### XRD analysis

The XRD analysis revealed that the average crystallite size of CuNPs synthesized using *R. stricta* was determined to be 15.95 nm (Figure 7).

#### Zeta potential of CuNPs

As shown in Figure 8, the zeta potential of the synthesized CuNPs was 42 mV. In this regard, zeta potential is considered an important indicator of the stability of a colloid, as the magnitude of the zeta potential reflects the extent of electrostatic repulsion between the same species constituting that colloid. The value of 42 mV indicates that the prepared NPs exhibit good stability (Mali et al., 2020).

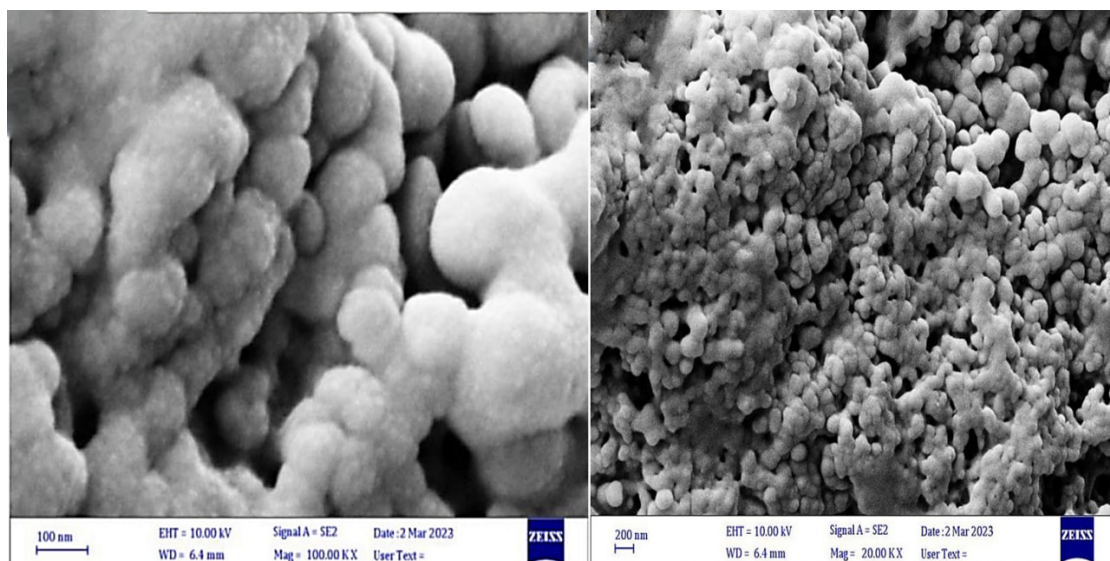


**Figure 4.** SEM analysis of NPs synthesized by *R. stricta* taken at different scales

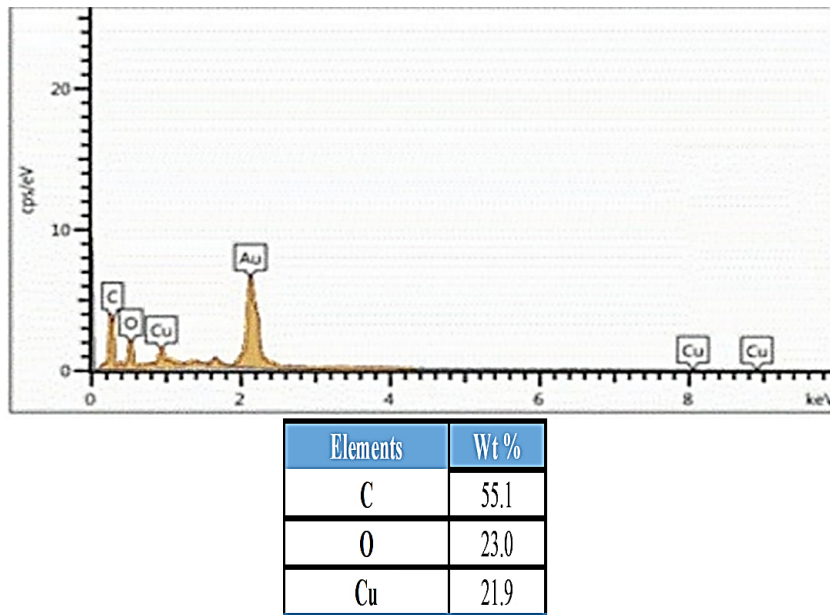


Figure 5. EDS analysis of biogenic NPs synthesized by *R. stricta*

Wound healing rate (%)

During the first to the fourth week of the research period, the healing rate of the wounded rabbits with *S. aureus* increased gradually ( $P < 0.05$ ). It varied significantly across the experimental treatments (Table 1).

Small letters indicate that means within the same column bearing different letters are significantly different at  $P < 0.05$ .

The highest rate of healing was seen in the CuNPs-treated group ( $100.75 \pm 1.41$ ), followed by the Fusidic acid-treated group ( $91.50 \pm 2.31$ ) (Xa-Bc-Biotech; China). Throughout the study, the CuNP treatment performed the best in terms of healing rate from the 1st week to the 4th week. These findings suggest that CuNPs expedite the healing of wounds.

Healing time

Table 2 displays the healing time required (in days) for the various treatments. The findings from the study revealed a statistically significant difference between the experimental treatments ( $P < 0.05$ ). During treatment, no adverse effects were observed in terms of the animal's body weight, overall health, or behavior.

Figure 9 shows images of the infected wounds treated with CuNPs for 0, 7, 14, and 21 days. Notably, after seven days of treatment, CuNPs successfully reduced the size and inflammation of the infected wounds. Re-epithelialization is vital in wound healing, as the skin performs a significant barrier function in protecting the body against pathogens (Zou et al., 2021).

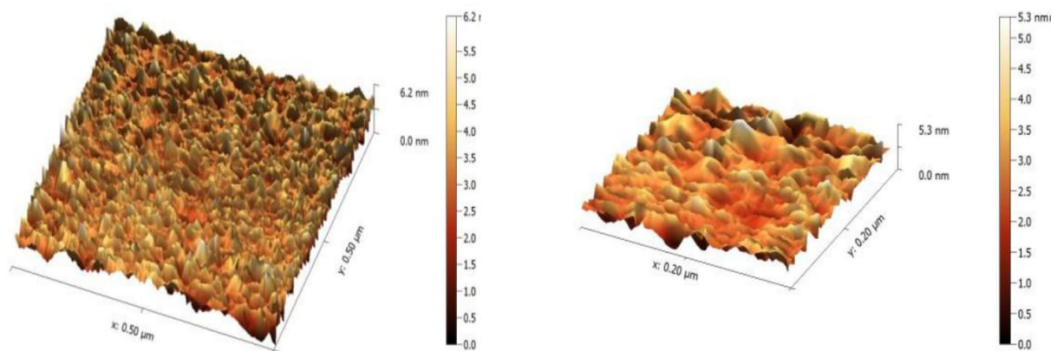


Figure 6. AFM analysis showing three-dimension images, and topography of biogenic CuNPs synthesized by *R. stricta*

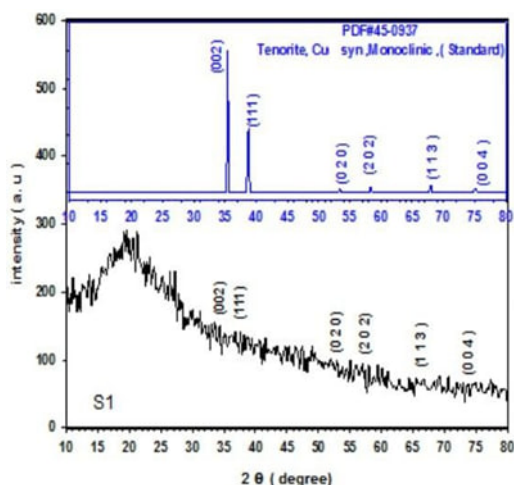


Figure 7. XRD pattern and quantitative analysis of the CuNPs synthesized by *R. stricta*

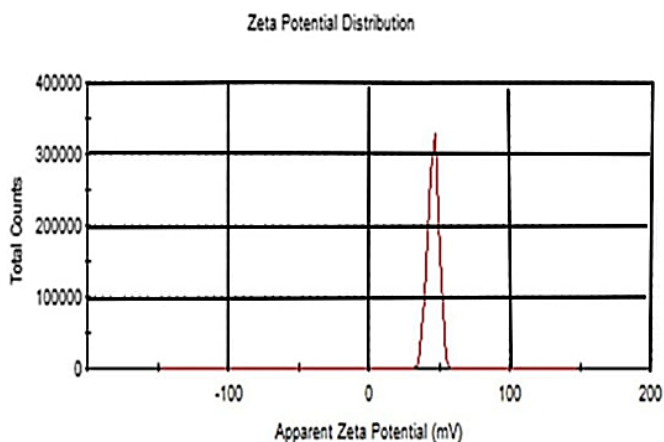


Figure 8. Zeta potential of the synthesized CuNP at 42 mV

After three and seven days, the untreated, infected wounds of the control group displayed significant inflammation (Figure 10).

**Hematological analysis**

The WBC count of the various treatments studied was significantly affected by the experimental groups ( $P < 0.05$ ), as shown in Table 3. The WBC count was con-

siderably increased in the non-treated/control group (at 0 and 28 days) compared to the treated group. Nevertheless, the treated group rebounded at the 14-, 21-, and 28-day intervals, with the seven-day interval showing the greatest increase.

Capital letters indicate that means within the same row bearing different letters are significantly different at  $P < 0.05$ .

Table 1. The effects of CuNPs and fusidic acid on the weekly rate of wound healing (percent) in rabbits

Treatment Groups	%			
	1 <sup>st</sup> Week	2 <sup>nd</sup> Week	3 <sup>rd</sup> Week	4 <sup>th</sup> Week
Group A (control) (No. 5)	31±1.68 <sup>Dc</sup>	45.75±0.95 <sup>Cc</sup>	63±1.97 <sup>Bc</sup>	76.5±2.82 <sup>Ac</sup>
CuNPs-treated group (No. 5)	52.25±1.59 <sup>Da</sup>	74±1.87 <sup>a</sup>	90.5±0.74 <sup>Ba</sup>	100.75±1.41 <sup>Aa</sup>
Fusidic acid-treated group (No. 5)	33.5±1.42 <sup>Db</sup>	53.25±3.45 <sup>Cb</sup>	69.25±2.96 <sup>Bb</sup>	91.5±2.31 <sup>Ab</sup>

<sup>A, B, C, D</sup>Significant difference within groups ( $P < 0.05$ ), <sup>a, b, c, d</sup>Significant difference between groups ( $P < 0.05$ ).



**Figure 9.** Digital images of wound healing taken on various days (0, 7, 14, and 21)

**Table 2.** The effects of CuNPs and fusidic acid on the rabbit's wound healing time at the 4<sup>th</sup> week

Treatment Groups	Healing Time (d)
Group (control) (No. 5)	32.00±0.40 <sup>A</sup>
CuNPs-treated group (No. 5)	16.25±0.47 <sup>C</sup>
Fusidic acid-treated group (No. 5)	22.25±0.75 <sup>B</sup>

<sup>A, B, C</sup>Significant difference between the groups (P<0.05).

Small letters indicate that means within the same column bearing different letters are significantly different at P<0.05.

### Bacterial counts

All treatment groups that received either CuNPs or fusidic acid successfully inhibited the development of *S. aureus*. The CuNPs-treated group could eradicate all bacterial cell-infected wounds in seven days, whereas the fusidic acid-treated group could eradicate all bacterial cell-infected wounds in 12 days (Table 4). This



**Figure 10.** Wounds infected in the control group

confirmed that CuNPs are a more effective antibacterial agent.

### Histological examination

The stained sections of healing wounds from the control group, the group treated with fusidic acid, and the group treated with CuNPs on various days are presented below. The examination was conducted using H&E staining at a magnification of 400x.

On the third day in the control group, it was observed that there was a loss of normal skin architecture with the absence of the epidermis. Also, the gap was filled with granulation tissue formation, accompanied by the infiltration of inflammatory cells. The sections that were stained in fusidic acid-treated wounds exhibited a greater infiltration of inflammatory cells and the deposition of edematous material, with a limited presence of fibroblasts. However, the group treated with CuNPs exhibited a lower level of inflammatory cell infiltration in comparison to the group treated with fusidic acid. Additionally, the presence of superficial necrotic tissue, along with edematous deposition and a limited number of fibroblasts, was observed (Figure 11).

On the seventh day, the wound sections of the control group exhibited a notable presence of inflammatory cells, suggesting that the inflammatory response re-

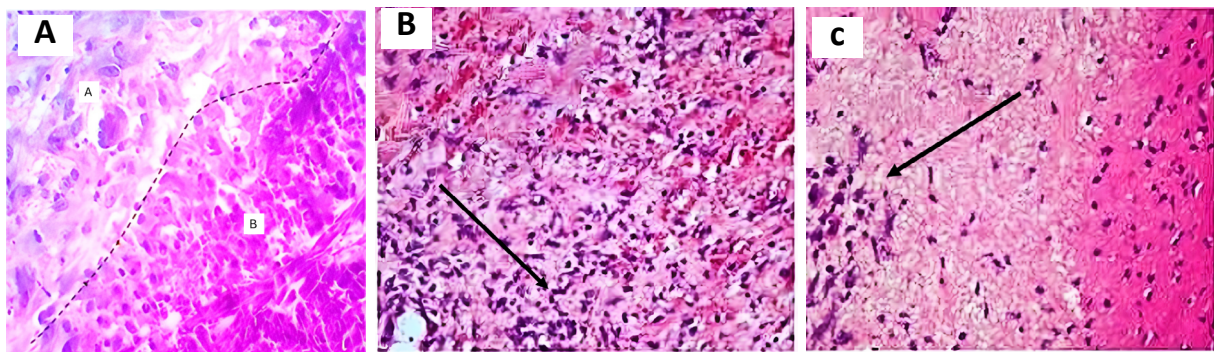


**Figure 11.** Histopathological evaluation of cutaneous wounds on day 3 in control, fusidic acid-treated, and CuNPs-treated groups

A) Histopathological characteristics of cutaneous wounds on day 3 in the untreated control group at the incision line, showing a demarcation line (dotted line) between (A) normal skin tissue and (B) granulation tissue with severe inflammatory cells (black arrow); B) Histopathological characteristics of cutaneous wounds on day 3 in the fusidic acid-treated group exhibited greater infiltration of inflammatory cells and deposition of edematous material, with a limited presence of fibroblasts; C) Histopathological characteristics of cutaneous wounds on day 3 in the CuNPs-treated group exhibited a lower level of inflammatory cell infiltration compared to the group treated with fusidic acid

mained uncontrolled. This could be attributed to the lack of antibacterial efficacy in the treatments administered. A notable inflammatory response was observed in the group that received Fusidic acid, which was accompanied by an increase in fibroblast proliferation. The experimental group that received CuNPs exhibited a mild inflammatory response, which was accompanied by an augmented proliferation of fibroblasts (Figure 12).

On the tenth day, the control group exhibited a substantial presence of inflammatory cells and an unhealed wound. The observations within the group administered with fusidic acid demonstrated resemblances to those within the control group. On the other hand, the group subjected to CuNPs demonstrated noteworthy fibroblast proliferation and the formation of well-organized blood vessels, along with collagen deposition (Figure 13).

On the fourteenth day, the control group demonstrated a significant presence of inflammatory cells, despite the absence of epithelial layer formation. On the other hand, the wounds that were treated with fusidic acid and CuNPs demonstrated the formation of a complete superficial epithelial layer along with the presence of well-established granulation tissue. The experimental group that received CuNPs demonstrated a more pronounced and mature superficial epithelial layer compared to the group that received fusidic acid. Additionally, a notable observation was made regarding the organization of collagen fibers in the group subjected to CuNPs treatment, which exhibited a significantly higher degree of organization in comparison to other groups (Figure 14).

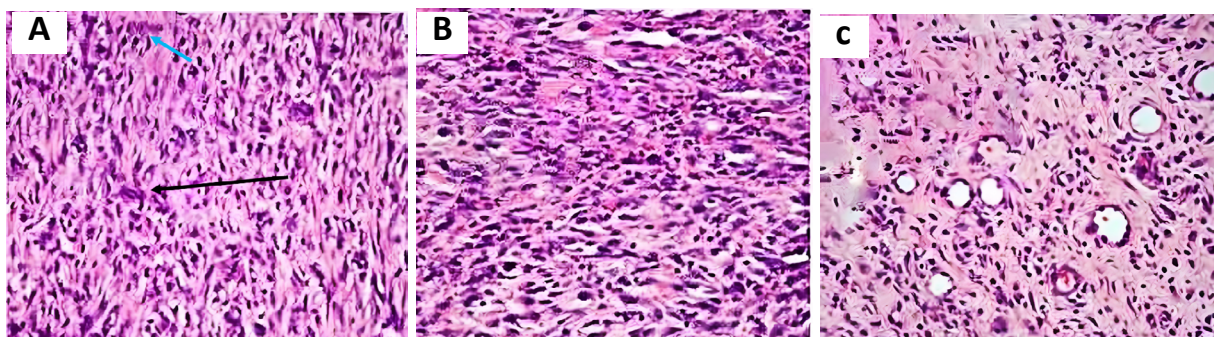


**Figure 12.** Histopathological evaluation of wound healing on day 7 in control, fusidic acid-treated, and CuNPs-treated groups

A) Histopathological characteristics of cutaneous wounds on day 7 in the untreated group, showing fibroblasts (black arrow) and blood vessels (blue arrow); B) Histopathological characteristics of cutaneous wounds on day 7 in the fusidic acid-treated groups; C) Histopathological characteristics of cutaneous wounds on day 7 in the CuNPs-treated group

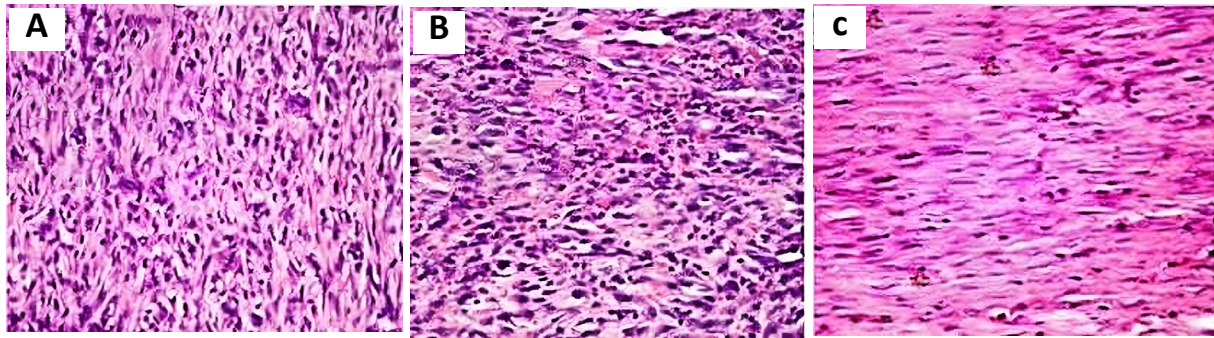


**Figure 13.** Histopathological evaluation of cutaneous wounds on day 10 in control, fusidic acid-treated, and CuNPs-treated groups

A) Histopathological characteristics of cutaneous wounds on day 10 in the untreated group; B) Histopathological characteristics of cutaneous wounds on day 10 in the fusidic acid group; C) Histopathological characteristics of cutaneous wounds on day 10 in the CuNPs-treated groups

## Discussion

The process of wound healing poses a significant challenge to researchers in the field. The process of wound healing commences with an initial inflammatory response, which is subsequently succeeded by the proliferation and migration of dermal and epidermal cells, as well as the synthesis of matrix components. These events collectively aim to bridge the wound gap and restore the integrity of the skin barrier (Alizadeh et al., 2019). In conclusion, the processes of tissue remodeling and differentiation facilitate a near-complete restoration of skin tissue and the re-establishment of its aesthetic properties (Hussain et al., 2022). The implementation of local therapy can effectively facilitate the healing process and mitigate the occurrence of systemic side effects (Wassif et al., 2021).

Wound contraction is a biological process, in which cells strategically arrange the extracellular matrix (ECM) of their surrounding tissue to expedite the healing process by minimizing the quantity of ECM that must be

generated. Wound contraction offers several advantages, primarily by expediting the healing process through the reduction of granulation tissue production required for tissue replacement (Zhang et al., 2022).

Considering the abovementioned, the assessment of wound contraction serves as a crucial method for determining the advancement of healing in cutaneous wounds. The observed increase in wound contraction in rabbits treated with CuNPs in the current study can be attributed to several factors, including enhanced fibroblast proliferation, increased collagen synthesis, and improved epithelialization. While the wound size reduction was observed in both the fusidic acid- and CuNPs-treated groups, the CuNPs-treated group exhibited a more pronounced effect. This suggests that CuNPs have a greater potential for enhancing the healing of cutaneous wounds compared to fusidic acid.

According to a study conducted by Tao et al., the application of CuNPs resulted in a significant reduction in the wound surface area in rabbits within the first day.

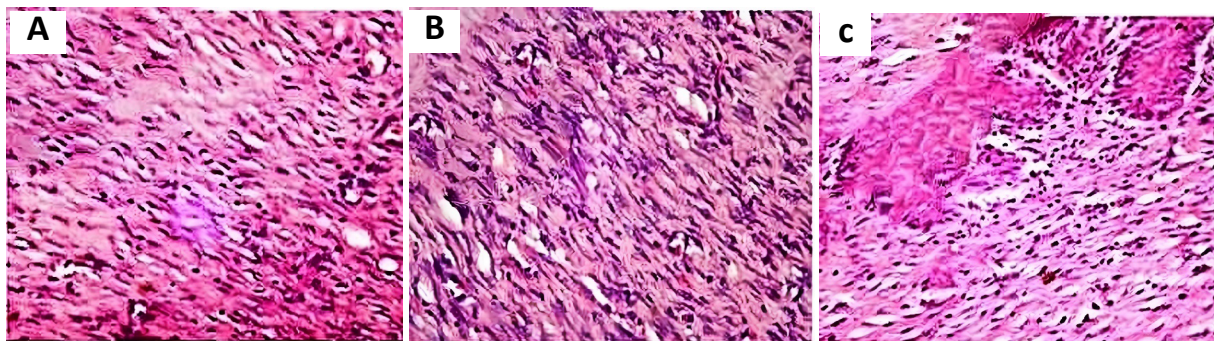


**Figure 14.** Histopathological evaluation of cutaneous wounds on day 14 in control, fusidic acid-treated, and CuNPs-treated groups

A) Histopathological characteristics of cutaneous wounds on day 14 in the untreated group; B) Histopathological characteristics of cutaneous wounds on day 14 in the fusidic acid-treated group; C) Histopathological characteristics of cutaneous wounds on day 14 in the CuNPs-treated group

**Table 3.** The effects of CuNPs and fusidic acid on the total number of white blood cells (cells/ $\mu$ L) in rabbits at weekly intervals

Treatment Groups	Day 0	1 <sup>st</sup> Week	2 <sup>nd</sup> Week	3 <sup>rd</sup> Week	4 <sup>th</sup> Week
Group A (control) (No. 5)	6700 $\pm$ 40.86 <sup>Ea</sup>	10775 $\pm$ 46.46 <sup>Da</sup>	1100 $\pm$ 45.49 <sup>Ca</sup>	11500 $\pm$ 51.02 <sup>Ba</sup>	11700 $\pm$ 43.69 <sup>Aa</sup>
CuNPs- treated group (No. 5)	5800 $\pm$ 46.26 <sup>Da</sup>	9000 $\pm$ 39.02 <sup>Ac</sup>	8200 $\pm$ 52.31 <sup>Bc</sup>	7400 $\pm$ 49.27 <sup>Cb</sup>	6000 $\pm$ 39.46 <sup>Db</sup>
Fusidic acid treated group) (No. 5)	6100 $\pm$ 45.26 <sup>Da</sup>	10300 $\pm$ 47.51 <sup>Ab</sup>	9500 $\pm$ 47.37 <sup>Bb</sup>	7600 $\pm$ 34.26 <sup>Cb</sup>	6300 $\pm$ 41.48 <sup>Db</sup>

A, B, C, D, E Significant difference within groups ( $P < 0.05$ ), a, b, c Significant difference between groups ( $P < 0.05$ ).

The contraction data observed within the 7–10-day time-frame demonstrated that CuNPs play a significant role in the proliferative phase (Tao et al., 2019).

The presence of inflammation in rabbits is commonly observed following a bacterial infection, resulting in an elevation in WBC count. The immune response of the host functions as a defensive mechanism that effectively combats bacterial invasion. The rise in WBCs is associated with the development of an infection caused by pathogenic bacteria, which in turn triggers the immune system to generate defensive cells. The significance of these cells in the body's immune response lies in their capacity to release immune chemicals that facilitate the eradication of microorganisms (Salem et al., 2020; Hossieni et al., 2021).

The groups treated with fusidic acid and CuNPs exhibited non-significant numbers of WBCs when infected with *S. aureus*. This suggests that CuNPs have a positive effect in counteracting the negative impact of bacteria and restoring the WBC count to normal levels.

*S. aureus* is a bacterium that belongs to the gram-positive category and is characterized by its anaerobic nature. The organism is widely acknowledged as a prominent causative agent of cutaneous infections, presenting a considerable risk to the overall well-being of the general population. The ability of *S. aureus* to endure oxidative substances plays a significant role in its ability to persist. Organisms in the logarithmic growth phase demonstrate a notable capacity to tolerate oxidative byproducts. The emergence of bacterial resistance in *S. aureus* presents

**Table 4.** Bacterial count prior to and following treatment

Treatment Groups	Day	Bacterial Count (CFU/10 $\mu$ L)
Group control (+) (No. 5)	3	1.4 $\times$ 10 <sup>10</sup>
	7	3.3 $\times$ 10 <sup>9</sup>
	9	6 $\times$ 10 <sup>9</sup>
CuNPs-treated group (No. 5)	3	4.2 $\times$ 10 <sup>5</sup>
	7	4.2 $\times$ 10 <sup>5*</sup>
	9	0*
	12	0*
	14	0*
Fusidic acid-treated group (No. 5)	3	6.2 $\times$ 10 <sup>5*</sup>
	7	5.1 $\times$ 10 <sup>5*</sup>
	9	4.1 $\times$ 10 <sup>5*</sup>
	12	0
	14	0

\*Significant differences at  $P < 0.001$  on days 3, 7, 9, 12, and 14 between the CuNPs, fusidic acid, and control groups.

significant obstacles in the management of infections attributed to this particular pathogen. The implementation of a preclinical animal model for *S. aureus* that is both efficient and cost-effective could offer an additional avenue for assessing the efficacy of antimicrobial agents (Treffon et al., 2020; Moradifar et al., 2024).

The pathogenic bacteria can be effectively inhibited through the utilization of CuNPs, owing to their capacity to traverse the bacterial cell membrane unhindered due to their small dimensions. This penetration of the cell membrane subsequently results in the degradation of essential components, such as minerals, proteins, and genetic material, ultimately leading to the demise of the bacterial cell. Moreover, it has been observed that CuNPs exhibit a potent antibacterial effect. Nevertheless, it is important to note that an excessive buildup of these NPs can lead to the demise of microbial cells (Gkanatsiou et al., 2019; Al-Garawi et al., 2022).

The utilization of the antibiotic fusidic acid, known for its wide-ranging antibacterial properties (Liu et al., 2020), likely leads to the inhibition of *S. aureus* and consequently promotes accelerated wound healing with no residual scarring observed in the group treated with fusidic acid. In contrast to the control group, the wounds that were treated with CuNPs or antibiotics exhibited the formation of a new layer of skin starting from day three, and the healing process was concluded by day 14 (Rafi et al., 2023). Rafi et al. assessed wound healing by evaluating various factors, including re-epithelialization, infiltration of inflammatory cells, regeneration and arrangement of collagen, as well as the presence of granulation tissue and skin appendages (Rafi et al., 2023).

Metal NPs typically infiltrate bacterial cells through an adsorption mechanism, leading to the release of metal ions that cause DNA damage and the generation of reactive oxygen species (ROS). This process results in a substantial increase in the surface area of bacterial cells, which subsequently interacts with intracellular enzymes (Abdelghany et al., 2023). The biopolymer is composed of carboxyl and amine groups, while copper typically forms interactions with these functional groups present on the surface of bacterial cells. The antibacterial efficacy of CuNPs is attributed to their ionic nature and surface charge. These NPs effectively interact with various functional groups present on the cell surface (Guan et al., 2021).

## Conclusion

The utilization of *R. stricta* leaf extract for the biosynthesis of CuNPs is demonstrated to be a straightforward,

environmentally sustainable, efficient, and economically viable method of synthesis. Nano copper has the potential to serve as an alternative therapeutic approach for treating wounds that are infected with *S. aureus*. This is due to the demonstrated ability of CuNPs to facilitate the healing process by exerting antibacterial and anti-inflammatory effects. At the histological level, the group treated with CuNPs exhibited a more rapid healing process characterized by complete re-epithelialization of the epidermis, significant fibroblastic activity, formation of dermal granulation tissue rich in collagen, and minimal infiltration of inflammatory cells.

## Ethical Considerations

### Compliance with ethical guidelines

The current study was carried out in accordance with the guidelines set forth by the Animal Ethics Committee of the Faculty of Veterinary Medicine at the University of Kufa, Kufa, Iraq, adhering to the regulations outlined in the granted license (Approval No.: 16881; Dated 12/7/2023)

### Funding

No external funds were received to complete this study.

### Authors' contributions

The authors significantly and directly contributed to the research and provided their consent for its publication.

### Conflict of interest

The authors reported no conflict of interest.

### Acknowledgments

The authors express their gratitude for the ethical support provided by the Faculty of Veterinary Medicine, University of Kufa, Kufa, Iraq.

## References:

- Abdelghany, T. M., Al-Rajhi, A. M. H., Yahya, R., Bakri, M. M., Al Abboud, M. A., & Yahya, R., et al. (2023). Phytofabrication of zinc oxide nanoparticles with advanced characterization and its antioxidant, anticancer, and antimicrobial activity against pathogenic microorganisms. *Biomass Conversion and Biorefinery*, 13, 417-430. [DOI:10.1007/s13399-022-03412-1]

- Alizadeh, S., Seyedalipour, B., Shafieyan, S., Kheime, A., Mohammadi, P., & Aghdami, N. (2019). Copper nanoparticles promote rapid wound healing in acute full thickness defect via acceleration of skin cell migration, proliferation, and neovascularization. *Biochemical and Biophysical Research Communications*, 517(4), 684-690. [DOI:10.1016/j.bbrc.2019.07.110] [PMID]
- Al-Mousaw, M., Bustani, G. S., Barqaawee, M. J. A., & Al-Shamma, Y. M. (2022). Evaluation of histology and sperm parameters of testes treated by lycopene against cyclophosphamide that induced testicular toxicity in Male rats. *AIP Conference Proceedings*, 2386(1). [DOI:10.1063/5.0067059]
- Al-Garawi, N. A. H. D., Suhail, A. A., Kareem, H. A., & Bustani, G. S. (2022). Study of Lipid Profile and Leptin hormone and Adiponectin hormone hypertensive patients in Najaf Governorate. *Revista Electronica de Veterinaria*, 23(3), 45-51. [Link]
- Awwad, A. M., Salem, N. M., & Abdeen, A. O. (2013). Green synthesis of silver nanoparticles using carob leaf extract and its antibacterial activity. *International Journal of Industrial Chemistry*, 4(29), 1-6. [Link]
- Badri, A., Slimi, S., Guergueb, M., Kahri, H., & Mateos, X. (2021). Green synthesis of copper oxide nanoparticles using Prickly Pear peel fruit extract: Characterization and catalytic activity. *Inorganic Chemistry Communications*, 134, 109027. [DOI:10.1016/j.inoche.2021.109027]
- Behera, S. S., Nath, I., Nayak, S., Parija, S. C., Mishra, U. K., & Kundu, A. K., et al. (2019). Histomorphological study of cutaneous wound healing in rabbits using xenogenic adipose derived stem cells. *Journal of Animal Research*, 9(5), 645-652. [DOI:10.30954/2277-940X.05.2019.3]
- Bukhari, S. I., Hamed, M. M., Al-Agamy, M. H., Gazwi, H. S., Radwan, H. H., & Youssif, A. M. (2021). Biosynthesis of copper oxide nanoparticles using *Streptomyces* MHM38 and its biological applications. *Journal of Nanomaterials*, 2021(1), 6693302. [DOI:10.1155/2021/6693302]
- Bustani, G. S., & Kashef Alghetaa, H. (2024). Exploring the Impact of Aryl Hydrocarbon Receptor (AhR) modulation on the blood-testis barrier integrity via tight junction protein-1 function. *Iranian Journal of Veterinary Medicine*. [Unpublished]. [Link]
- Cardoso, C. G., Ayer, I. M., Jorge, A. T., Honsho, C. S., & Mattos-Junior, E. (2020). A comparative study of the cardiopulmonary and sedative effects of a single intramuscular dose of ketamine anesthetic combinations in rabbits. *Research in Veterinary Science*, 128, 177-182. [DOI:10.1016/j.rvsc.2019.11.016] [PMID]
- Caroling, G., Tiwari, S. K., Ranjitham, A. M., & Suja, R. (2013). Biosynthesis of silver nanoparticles using aqueous broccoli extract-characterization and study of antimicrobial, cytotoxic effects. *Asian Journal of Pharmaceutical and Clinical Research*, 6(4), 165-172. [Link]
- Chinnathambi, A., Awad Alahmadi, T., & Ali Alharbi, S. (2021). Biogenesis of copper nanoparticles (Cu-NPs) using leaf extract of *Allium noeanum*, antioxidant and in-vitro cytotoxicity. *Artificial Cells, Nanomedicine, and Biotechnology*, 49(1), 500-510. [DOI:10.1080/21691401.2021.1926275] [PMID]
- Diniz, F. R., Maia, R. C. A. P., Rannier, L., Andrade, L. N., V Chaud, M., & da Silva, C. F., et al. (2020). Silver nanoparticles-composing alginate/gelatine hydrogel improves wound healing in vivo. *Nanomaterials (Basel, Switzerland)*, 10(2), 390. [DOI:10.3390/nano10020390] [PMID]
- Foroutan, S., Eslampour, M. A., Emaneini, M., Jabalameli, F., & Akbari, G. (2022). Characterization of biofilm formation ability, virulence factors and antibiotic resistance pattern of staphylococcus aureus isolates from subclinical bovine mastitis. *Iranian Journal of Veterinary Medicine*, 16(2), 144-154. [Link]
- Gaddafi, M. S., Yakubu, Y., Junaidu, A. U., Bello, M. B., Bitrus, A. A., & Musawa, A. I., et al. (2023). Occurrence of Methicillin-resistant *Staphylococcus aureus* (MRSA) from dairy cows in Kebbi, Nigeria. *Iranian Journal of Veterinary Medicine*, 17(1), 19-26. [DOI:10.22059/ijvm.17.1.1005256]
- Gkanatsiou, C., Karamanoli, K., Menkissoglu-Spiroudi, U., & Dendrinou-Samara, C. (2019). Composition effect of Cu-based nanoparticles on phytopathogenic bacteria. Antibacterial studies and phytotoxicity evaluation. *Polyhedron*, 170, 395-403. [DOI:10.1016/j.poly.2019.06.002]
- Guan, G., Zhang, L., Zhu, J., Wu, H., Li, W., & Sun, Q. (2021). Antibacterial properties and mechanism of biopolymer-based films functionalized by CuO/ZnO nanoparticles against *Escherichia coli* and *Staphylococcus aureus*. *Journal of Hazardous Materials*, 402, 123542. [DOI:10.1016/j.jhazmat.2020.123542] [PMID]
- Hasanin, M., Al Abboud, M. A., Alawlaqi, M. M., Abdelghany, T. M., & Hashem, A. H. (2022). Ecofriendly synthesis of biosynthesized copper nanoparticles with starch-based nanocomposite: Antimicrobial, antioxidant, and anticancer activities. *Biological Trace Element Research*, 200(5), 2099-2112. [DOI:10.1007/s12011-021-02812-0] [PMID]
- Hussain, Z., Thu, H. E., Rawas-Qalaji, M., Naseem, M., Khan, S., & Sohail, M. (2022). Recent developments and advanced strategies for promoting burn wound healing. *Journal of Drug Delivery Science and Technology*, 68, 103092. [DOI:10.1016/j.jddst.2022.103092]
- Hossieni, M., Kiani, S. J., Tavakoli, A., Kachoei, A., Habib, Z., & Monavari, S. H. (2024). In vitro inhibition of rotavirus multiplication by copper oxide nanoparticles. *Archives of Razi Institute*, 79(1), 83-91. [DOI:10.32592/ARI.2024.79.1.83] [PMID]
- Islam, F., Shohag, S., Uddin, M. J., Islam, M. R., Nafady, M. H., & Akter, A. S., et al. (2022). Exploring the journey of zinc oxide nanoparticles (ZnO-NPs) toward biomedical applications. *Materials*, 15(6), 2160. [DOI:10.3390/ma15062160] [PMID]
- Liu, L., Shen, X., Yu, J., Cao, X., Zhan, Q., & Guo, Y., et al. (2020). Subinhibitory concentrations of fusidic acid may reduce the virulence of *S. aureus* by down-regulating sara and saers to reduce biofilm formation and  $\alpha$ -toxin expression. *Frontiers in Microbiology*, 11, 25. [DOI:10.3389/fmicb.2020.00025] [PMID]
- Mali, S. C., Dhaka, A., Githala, C. K., & Trivedi, R. (2020). Green synthesis of copper nanoparticles using *Celastrus paniculatus* Willd. leaf extract and their photocatalytic and antifungal properties. *Biotechnology Reports*, 27, e00518. [DOI:10.1016/j.btre.2020.e00518] [PMID]
- Mirnezami, M., Rahimi, H., Fakhar, H. E., & Rezaei, K. (2018). The role of topical estrogen, phenytoin, and silver sulfadiazine in time to wound healing in rats. *Ostomy/Wound Management*, 64(8), 30-34. [PMID] [DOI:10.26855/ijcemr.2023.04.023]

- Moradifar, N., Moayyedkazemi, A., Mohammadi, H., Ahmadi, S., & Raziani, Y. (2024). Investigating the potential application of organic and inorganic nanoparticles for gastric cancer treatment: An evidence-based review. *Archives of Razi Institute*, 79(2), 264-271. [DOI:10.32592/ARI.2024.79.2.264] [PMID]
- Pal, M., Shuramo, M. Y., Tewari, A., Srivastava, J. P., & Steinmetz, C. H. (2023). Staphylococcus aureus from a commensal to zoonotic pathogen: A critical appraisal. *International Journal of Clinical and Experimental Medicine Research*, 7(2), 220-228. [Link]
- Rafi, R., Zulfiqar, S., Asad, M., Zeeshan, R., Zehra, M., & Khalid, H., et al. (2023). Smart wound dressings based on carbon doped copper nanoparticles for selective bacterial detection and eradication for efficient wound healing application. *Materials Today Communications*, 35, 105914. [DOI:10.1016/j.mtcomm.2023.105914]
- Rahman, H., Rauf, A., Khan, S. A., Ahmad, Z., Alshammari, A., & Alharbi, M., et al. (2023). Green synthesis of silver nanoparticles using rhazya stricta decne extracts and their anti-microbial and anti-oxidant activities. *Crystals*, 13(3), 398. [DOI:10.3390/cryst13030398]
- Rahchamani, R., Zarooni, S., & Borhani, M. S. (2024). The chemical composition and antibacterial effect of essential oils of rosemary and basil in milk. *Iranian Journal of Veterinary Medicine*. [Unpublished]. [Link]
- Raja, S., Ramesh, V., & Thivaharan, V. (2017). Green biosynthesis of silver nanoparticles using Calliandra haematocephala leaf extract, their antibacterial activity and hydrogen peroxide sensing capability. *Arabian Journal of Chemistry*, 10(2), 253-261. [DOI:10.1016/j.arabj.2015.06.023]
- Rani, R., Sharma, D., Chaturvedi, M., & Yadav, J. P. (2020). Green synthesis of silver nanoparticles using Tridax procumbens: their characterization, antioxidant and antibacterial activity against MDR and reference bacterial strains. *Chemical Papers*, 74, 1817-1830. [DOI:10.1007/s11696-019-01028-w]
- Razdan, K., Garcia-Lara, J., Sinha, V. R., & Singh, K. K. (2022). Pharmaceutical strategies for the treatment of bacterial biofilms in chronic wounds. *Drug Discovery Today*, 27(8), 2137-2150. [DOI:10.1016/j.drudis.2022.04.020] [PMID]
- Salem, M. I., El-Sebai, A., Elnagar, S. A., & Abd El-Hady, A. M. (2020). WITHDRAWN: Evaluation of lipid profile, antioxidant and immunity statuses of rabbits fed Moringa oleifera leaves. *Asian-Australasian Journal of Animal Sciences*, 10.5713/ajas.20.0499. Advance online publication. [DOI:10.5713/ab.20.0499] [PMID]
- Samuel, M. S., Ravikumar, M., John J, A., Selvarajan, E., Patel, H., & Chander, P. S., et al. (2022). A review on green synthesis of nanoparticles and their diverse biomedical and environmental applications. *Catalysts*, 12(5), 459. [DOI:10.3390/catal12050459]
- Sato, H., Ebisawa, K., Takanari, K., Yagi, S., Toriyama, K., Yamawaki-Ogata, A., & Kamei, Y. (2015). Skin-derived precursor cells promote wound healing in diabetic mice. *Annals of Plastic Surgery*, 74(1), 114-120 [DOI:10.1097/SAP.0000000000000342] [PMID]
- Tanideh, N., Rokhsari, P., Mehrabani, D., Mohammadi Samani, S., Sabet Sarvestani, F., & Ashraf, M. J., et al. (2014). The healing effect of licorice on Pseudomonas aeruginosa infected burn wounds in experimental rat model. *World Journal of Plastic Surgery*, 3(2), 99-106. [PMID]
- Tao, B., Lin, C., Deng, Y., Yuan, Z., Shen, X., & Chen, M., et al. (2019). Copper-nanoparticle-embedded hydrogel for killing bacteria and promoting wound healing with photothermal therapy. *Journal of Materials Chemistry B*, 7(15), 2534-2548. [PMID]
- Treffon, J., Chaves-Moreno, D., Niemann, S., Pieper, D. H., Vogl, T., & Roth, J., et al. (2020). Importance of superoxide dismutases A and M for protection of Staphylococcus aureus in the oxidative stressful environment of cystic fibrosis airways. *Cellular Microbiology*, 22(5), e13158. [DOI:10.1111/cmi.13158] [PMID]
- Vinelli, A., Primiceri, E., Brucale, M., Zuccheri, G., Rinaldi, R., & Samori, B. (2008). Sample preparation for the quick sizing of metal nanoparticles by atomic force microscopy. *Microscopy Research and Technique*, 71(12), 870-879. [DOI:10.1002/jemt.20631] [PMID]
- Wassif, R. K., Elkayal, M., Shamma, R. N., & Elkheshen, S. A. (2021). Recent advances in the local antibiotics delivery systems for management of osteomyelitis. *Drug Delivery*, 28(1), 2392-2414. [DOI:10.1080/10717544.2021.1998246] [PMID]
- Xiao, H., Chen, X., Liu, X., Wen, G., & Yu, Y. (2023). Recent advances in decellularized biomaterials for wound healing. *Materials Today. Bio*, 19, 100589. [DOI:10.1016/j.mt-bio.2023.100589] [PMID]
- Yaşayan, G., Nejati, O., Ceylan, A. F., Karasu, Ç., Ugur, P. K., & Bal-Öztürk, A., et al. (2023). Tackling chronic wound healing using nanomaterials: advancements, challenges, and future perspectives. *Applied Materials Today*, 32, 101829. [DOI:10.1016/j.apmt.2023.101829]
- Zhang, Q., Wang, P., Fang, X., Lin, F., Fang, J., & Xiong, C. (2022). Collagen gel contraction assays: From modelling wound healing to quantifying cellular interactions with three-dimensional extracellular matrices. *European Journal of Cell Biology*, 101(3), 151253. [DOI:10.1016/j.ejcb.2022.151253] [PMID]
- Zhang, W., Roy, S., & Rhim, J. W. (2023). Copper-based nanoparticles for biopolymer-based functional films in food packaging applications. *Comprehensive Reviews in Food Science and Food Safety*, 22(3), 1933-1952. [DOI:10.1111/1541-4337.13136]
- Zhao, H., Maruthupandy, M., Al-mekhlafi, F. A., Chackaravarthi, G., Ramachandran, G., & Chelliah, C. K. (2022). Biological synthesis of copper oxide nanoparticles using marine endophytic actinomycetes and evaluation of biofilm producing bacteria and A549 lung cancer cells. *Journal of King Saud University-Science*, 34(3), 101866. [DOI:10.1016/j.jksus.2022.101866]
- Zou, M. L., Teng, Y. Y., Wu, J. J., Liu, S. Y., Tang, X. Y., & Jia, Y., et al. (2021). Fibroblasts: Heterogeneous cells with potential in regenerative therapy for scarless wound healing. *Frontiers in Cell and Developmental Biology*, 9, 713605. [DOI:10.3389/fcell.2021.713605] [PMID]

This Page Intentionally Left Blank